JIPB Journal of Integrative Plant Biology

A bestrophin-like protein modulates the proton motive force across the thylakoid membrane in *Arabidopsis*

Zhikun Duan[1,2†], Fanna Kong[1,2†], Lin Zhang[1,2], Wenjing Li[1], Jiao Zhang[1] and Lianwei Peng[1*]

[1]Key Laboratory of Photobiology, CAS Center for Excellence in Molecular Plant Sciences, Institute of Botany, Chinese Academy of Sciences, Beijing 100093, China, [2]University of Chinese Academy of Sciences, Beijing 100049, China. [†]These authors contributed equally to this work. *Correspondence: penglianwei@ibcas.ac.cn

Abstract During photosynthesis, photosynthetic electron transport generates a proton motive force (pmf) across the thylakoid membrane, which is used for ATP biosynthesis via ATP synthase in the chloroplast. The pmf is composed of an electric potential ($\Delta\Psi$) and an osmotic component (ΔpH). Partitioning between these components in chloroplasts is strictly regulated in response to fluctuating environments. However, our knowledge of the molecular mechanisms that regulate pmf partitioning is limited. Here, we report a bestrophin-like protein (AtBest), which is critical for pmf partitioning. While the ΔpH component was slightly reduced in *atbest*, the $\Delta\Psi$ component was much greater in this mutant than in the wild type, resulting in less efficient activation of nonphotochemical quenching (NPQ) upon both illumination and a shift from low light to high light. Although no visible phenotype was observed in the *atbest* mutant in the greenhouse, this mutant exhibited stronger photoinhibition than the wild type when grown in the field. AtBest belongs to the bestrophin family proteins, which are believed to function as chloride (Cl^-) channels. Thus, our findings reveal an important Cl^- channel required for ion transport and homeostasis across the thylakoid membrane in higher plants. These processes are essential for fine-tuning photosynthesis under fluctuating environmental conditions.

Keywords: Bestrophin; Cl^- channel; photoprotection; photosynthesis; proton motive force
Citation: Duan Z, Kong F, Zhang L, Li W, Zhang J, Peng L (2016) A bestrophin-like protein modulates the proton motive force across the thylakoid membrane in *Arabidopsis*. **J Integr Plant Biol** XX: XX–XX doi: 10.1111/jipb.12475
Edited by: Chun-Ming Liu, Institute of Botany, CAS, China
Received Mar. 1, 2016; **Accepted** Mar. 3, 2016
Available online on Mar. 7, 2016 at www.wileyonlinelibrary.com/journal/jipb

Research Article

OnlineOpen

INTRODUCTION

In the 1960s, Mitchell proposed that respiratory and light-induced photosynthetic electron transport are coupled with proton (H^+) transport across the mitochondrial inner membrane and chloroplast thylakoid membrane, thus generating a proton motive force (pmf) used to drive ATP synthase and produce ATP (Mitchell 1966). According to this hypothesis, the pmf is composed of two components, the transmembrane proton gradient (ΔpH) and the electric field gradient ($\Delta\Psi$), which are thermodynamically equivalent (Mitchell 1961, 1966). Due to the low permeability of the inner mitochondrial membrane to ions, $\Delta\Psi$ is the predominant component of the pmf, while the contribution of ΔpH is smaller, as ΔpH across this membrane is only approximately 0.5 (Mitchell 1966). However, the contribution of ΔpH to pmf is significantly higher in chloroplasts, where the ΔpH across thylakoid membrane is thought to be approximately 2.0 (with a lumen pH $>$ 5.8) during photosynthesis (Kramer et al. 2003). It has been suggested that approximately 50% of the pmf can be stored as $\Delta\Psi$ (Cruz et al. 2001). In addition, the pmf has also been proposed to be stored almost entirely as ΔpH in the chloroplast (Johnson and Ruban 2014). In both cases, the $\Delta\Psi$ must be dissipated rapidly to maintain high proton levels in the thylakoid lumen, which is essential for activating energy-dependent nonphotochemical quenching (NPQ) of absorbed excess light, and for restricting photosynthetic electron transport under high light or CO_2-limited conditions in higher plants (Hope et al. 1994; Niyogi 1999).

Numerous electrophysiological studies using the thylakoid membrane have demonstrated that ion counterbalancing via the influx of anions (such as chloride (Cl^-)) and efflux of cations (such as potassium (K^+) and magnesium (Mg^{2+})) across the thylakoid membrane is essential for $\Delta\Psi$ dissipation (Hind et al. 1974; Schönknecht et al. 1988; Pottosin and Schönknecht 1996). However, the molecular machinery responsible for ion movement has long been unclear. Recently, Carraretto et al. (2013) identified a two-pore K^+ channel, AtTPK3, which is essential for light utilization and dissipation. AtTPK3 is located on the stroma thylakoid and is activated by Ca^{2+} and a high concentration of H^+. Electrochromic shift (ECS) analysis revealed an increase in $\Delta\Psi$ and a decrease in ΔpH in *TPK3*-silenced *Arabidopsis thaliana* plants (Carraretto et al. 2013), indicating that TPK3 is involved in pmf

partitioning through mediating efflux of K^+ from the thylakoid lumen during photosynthesis. In cyanobacteria, a six transmembrane-domain K^+ channel, SynK, modulates the balance between $\Delta\Psi$ and ΔpH (Checchetto et al. 2012). Both *TPK3*-silenced *Arabidopsis* plants and the SynK-less cyanobacterial mutant have enhanced photosensitivity under high light intensities (Checchetto et al. 2012; Carraretto et al. 2013). KEA3 is a H^+/K^+ antiporter present in the thylakoid membrane that is thought to mediate H^+ efflux from the thylakoid lumen and K^+ influx from the chloroplast stroma under certain conditions, such as a shift from high light to low light (Armbruster et al. 2014; Kunz et al. 2014). Not only does KEA3 replenish K^+ levels in the thylakoid lumen, but it also accelerates downregulation of NPQ via a rapid efflux of H^+ after a transition to low light (Armbruster et al. 2014). Therefore, K^+ channels and H^+/K^+ antiporters in the thylakoid form an intricate network that mediates K^+ transport across the thylakoid and fine-tunes photosynthesis in response to fluctuating environments.

In addition to K^+ channels, Cl^- channel activity has also been detected in the thylakoid membranes of higher plants and algae (Schönknecht et al. 1988; Pottosin and Schönknecht 1995, 1996). Of the seven Cl^- channel (CLC) proteins encoded by the *Arabidopsis* genome, only one, ClCe, is located in the thylakoid membrane (Marmagne et al. 2007; Lv et al. 2009; Barbier-Brygoo et al. 2011). However, ClCe does not contain a selectivity motif for Cl^- transport (Barbier-Brygoo et al. 2011) and it was proposed that ClCe transports NO_3^- instead of Cl^- (Monachello et al. 2009). Thus, it is unclear what type of Cl^- channel/transporter is responsible for the Cl^- channel activity in photosynthetic membranes, although this activity was detected almost 30 years ago (Schönknecht et al. 1988; Pottosin and Schönknecht 1995, 1996).

Bestrophin family proteins are believed to function as Ca^{2+}-activated Cl^- channels in mammalian cells (Sun et al. 2002; Dickson et al. 2014). The first reported bestrophin gene, *VMD2*, was discovered in human; several point mutations in this gene (which encodes hBest1) cause Best vitelliform macular dystrophy (Petrukhin et al. 1998). Recently, high-resolution crystal structures of chicken Best1 (cBest1) and the Best complex from *Klebsiella pneumoniae* (KpBest) were resolved at 2.85 Å and 2.3 Å, respectively (Dickson et al. 2014; Yang et al. 2014). Both bestrophins form a stable pentamer, and each subunit has four transmembrane domains. Although cBest1 is a Ca^{2+}-activated Cl^- channel, the KpBest complex was proposed to be a cation channel (such as Na^+), and Ca^{2+} is not required for its activation (Dickson et al. 2014; Yang et al. 2014). These findings suggest that both the function and regulatory mechanism of bestrophin proteins have diversified during evolution.

In this study, we showed that a bestrophin-like protein (AtBest) from *Arabidopsis* reduces the $\Delta\Psi$ component of the pmf during photosynthesis. AtBest is a member of the bestrophin family and is located in the thylakoid membrane. Our results demonstrated that AtBest may represent a previously unknown ion channel responsible for Cl^- channel activity in photosynthetic membranes. This activity plays an important role in photoprotection for plants under fluctuating environmental conditions, as it counterbalances the flux of ions across the thylakoid and modulates the partitioning of the pmf.

RESULTS

Isolation and phenotype of the *atbest* mutant

The mutant *atbest1-1* was isolated from an ethyl methanesulfonate (EMS)-mutagenized *Arabidopsis* mutant pool constructed in our laboratory using an IMAGING-PAM fluorometer (Walz, Effeltrich, Germany) according to the low level of NPQ following a 40-s illumination (Figure 1). We designated this mutant *atbest1-1* because the mutated gene encodes a bestrophin family protein in *Arabidopsis*. As shown in Figure 1A and 1B, NPQ was transiently induced to approximately 0.8 within 40 s in WT plants during the dark-to-light (50 μmol photons $\cdot m^{-2} \cdot s^{-1}$) transition. However, NPQ levels were significantly lower ($\sim$0.5, $P < 0.01$, Student's *t*-test) after 40 s of illumination in *atbest1-1* compared to the WT (Figure 1A, B). Due to the activation of ATP synthase, NPQ is rapidly relaxed within 2 min of induction; similar levels of NPQ were found between WT and *atbest1-1* after 2 min of illumination (Figure 1A, B). Genetic mapping of the mutant gene revealed a single mutation (G-to-A) at nucleotide position 1,153 bp of the *At3g61320* (*AtBest1*) gene relative to the ATG codon, resulting in a premature stop codon (Figure 1E). To confirm that the mutation in *At3g61320* is responsible for the observed phenotype, we analyzed the T-DNA insertion line *atbest1-2* (Figure 1E). Reverse transcription (RT)-PCR analysis did not detect any transcripts for this allele after 35 cycles of PCR (Figure 1G), indicating that it is a null mutant. Both alleles exhibited the same phenotype during NPQ induction (Figure 1A).

A BLAST search revealed that the product of *At2g45870* (*AtBest2*) is a bestrophin-like protein that shares 76/85% sequence identity/similarity with AtBest1 (Figures S1, S2). Quantitative real-time PCR revealed that the expression level of *AtBest2* was only approximately 10% that of *AtBest1* in mature *Arabidopsis* leaves ($P < 0.01$, Student's *t*-test, Figure 1G), indicating that AtBest1 is the predominant form. Consistent with this finding, the T-DNA insertion mutant *atbest2-1* exhibited the same NPQ induction phenotype as the WT, and the phenotype of the *atbest1-1 atbest2-1* double mutant was similar to that of *atbest1* (Figure 1A, B). Furthermore, the double mutant overexpressing *AtBest1* or *AtBest2* exhibited accelerated NPQ activation kinetics and higher maximum NPQ levels compared with WT plants during the dark-to-light transition (Figure 1C), indicating that the phenotype of the double mutant can be fully restored by *AtBest1* or *AtBest2*. These results indicate that AtBest1 and AtBest2 have redundant functions in *Arabidopsis*. We used the double mutant *atbest1-1 atbest2-1* in subsequent experiments and designated this mutant *atbest*.

No visible phenotype was observed for *atbest* under our growth chamber conditions (Figure 1A, B). Blue native (BN)-PAGE and immunoblot analyses showed that the levels of major photosynthetic complexes such as photosystem II (PSII), PSI (PsaA and PsaD), Cyt b_6f (cytochrome b_6f complex), and ATP synthase were identical between *atbest* and the WT (Figure S3). The NDH (NADH dehydrogenase-like complex) and PGR5/PGRL1 complexes are involved in cyclic electron transport around PSI in higher plants. The levels of the subunits of these complexes, NdhH and PGRL1, were also not affected in *atbest*. The thylakoid protein PsbS is essential for qE activation; similar levels of PsbS were detected in *atbest*

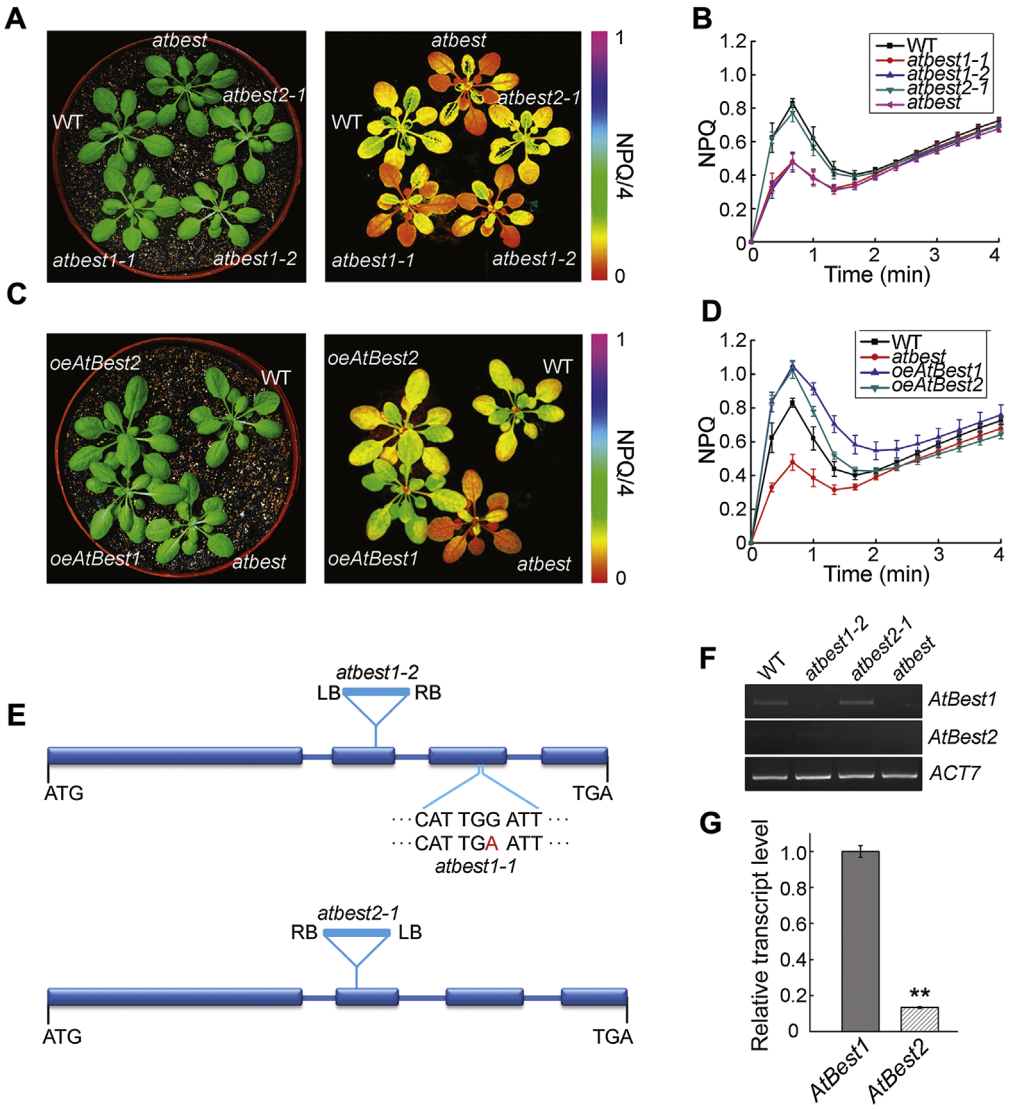

Figure 1. Identification and characterization of the *atbest* mutants

(A, C) Growth and nonphotochemical quenching (NPQ) phenotypes of the *atbest* mutants. Four-week-old plants grown on soil at 80 μmol photons $\cdot m^{-2} \cdot s^{-1}$ (left panels). The photosynthetic parameter NPQ was measured upon illumination for 40 s using an Imaging PAM system (right panels). Signal intensities for NPQ/4 are indicated according to the color scale (0 to 1.0) on the right. WT, wild type; *atbest*, *atbest1-1 atbest2-1* double mutant; *oeAtBest1* and *oeAtBest2*, *atbest* mutant complemented with the CDS of *AtBest1* and *AtBest2*, respectively, under the control of the CaMV 35S promoter. **(B, D)** NPQ induction curves of the *atbest* mutants and wild-type plants. NPQ was calculated as (Fm-Fm')/Fm'. Data are presented as the means ± *SD* ($n = 3$). **(E)** Schematic representation of *AtBest1* and *AtBest2* and the positions of the T-DNA insertions and single mutation. **(F)** RT-PCR analysis of transcript levels of *AtBest* in the mutants. *ACT7* was used as a control. **(G)** Transcript abundance of *AtBest1* and *AtBest2* by real-time quantitative RT-PCR. Error bars indicate ±SD ($n = 3$). Asterisks indicate the expression level of *AtBest1* and *AtBest2* differ significantly (**$P < 0.01$, Student's *t*-test).

and WT plants (Figure S3). These results indicate that AtBest is not required for the accumulation of thylakoid complexes and factors involved in cyclic electron transport and NPQ induction.

AtBest localizes to the stroma thylakoid in chloroplasts

Both AtBest proteins are predicted to have a chloroplast localization signal peptide in their N-termini, suggesting that they are localized to the chloroplast (Figures 2A, S1). To confirm this hypothesis, GFP (green fluorescent protein)-tagged AtBest fusion proteins were expressed in protoplasts (Figure 2B). AtBest-GFP fluorescence exclusively co-localized with chloroplasts, but its fluorescence pattern differed from that of GFP fused with Tic20, a chloroplast envelope protein, which produced ring-shaped signals surrounding the central red chlorophyll fluorescence signal (Figure 2B). These results suggest that AtBest is a chloroplast protein that is not localized to the chloroplast envelope. To further investigate

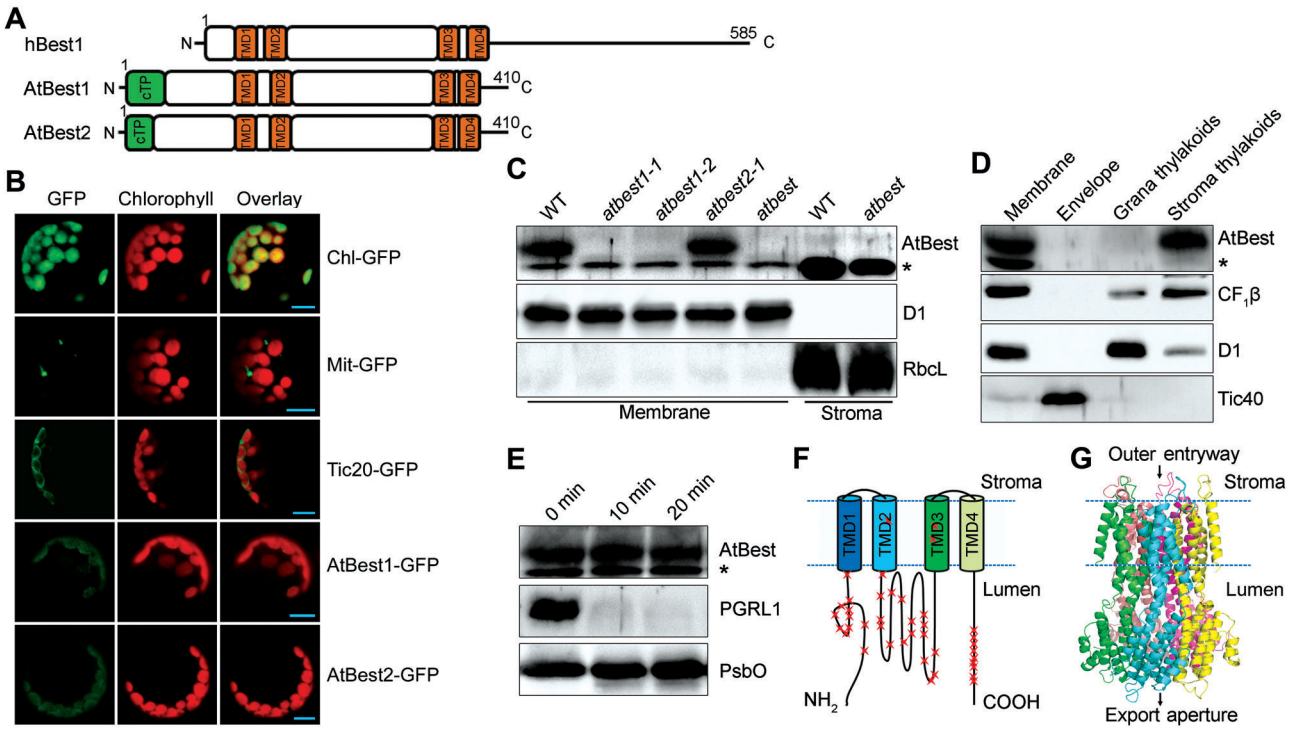

Figure 2. AtBest is localized to the stroma thylakoid in chloroplasts

(A) Schematic protein structure of hBest1, AtBest1, and AtBest2. Chloroplast-targeting peptide (cTP) and transmembrane domains are indicated by green and brown boxes, respectively. **(B)** Subcellular localization of AtBest by GFP assay. AtBest1-GFP, AtBest1-GFP fusion; AtBest2-GFP, AtBest2-GFP fusion; Chl-GFP, chloroplast control; Mit-GFP, mitochondrial control; Tic20-GFP, Tic20-GFP fusion as a chloroplast envelope localization control. Bars = 5 μm. **(C, D)** Immunolocalization analysis of AtBest. Intact chloroplasts isolated from various genotypes were fractionated into membrane and stromal fractions, and immunoblot analyses were performed. D1 and RbcL were used as loading and fractionation controls (**C**). Total chloroplast membrane was further separated into envelope membrane, grana thylakoids, and stroma thylakoids, and immunoblot analysis was performed with specific antibodies against AtBest, D1, $CF_1\beta$, and Tic40 (**D**). *Non-specific signal. **(E)** Trypsin digestion analysis. Immunoblot analysis of AtBest, PGRL1, and PsbO in thylakoids before (0 min) and after (10 and 20 min) treatment with trypsin (10 μg/mL). **(F)** Schematic representation of the topology of AtBest in the thylakoid. Trypsin cleavage sites in AtBest1 are indicated by asterisks. **(G)** The tertiary structure of the AtBest channel predicted by SwissModel using KpBest as template.

the precise localization of AtBest in chloroplasts, we raised a specific polyclonal antibody against AtBest. Signals from a protein with a molecular mass of approximately 37 kDa were detected in the membrane fractions of WT and *atbest2-1*, but they were absent in the membrane fractions of *atbest1-1*, *atbest1-2*, and *atbest* as well as in the stromal fractions of WT and *atbest* plants (Figure 2C), implying that AtBest is a membrane protein. Further subfractionation of the chloroplast membrane and immunoblot analysis demonstrated that AtBest1 is mainly localized to the stroma thylakoid (Figure 2D).

AtBest was predicted to have four transmembrane domains (TMD1-4) and to lack the long but diverse C-terminal domain present in animal bestrophins (Figures 2A, S1). This C-terminal domain is believed to mediate protein–protein interactions (Milenkovic et al. 2008). To determine the topology of AtBest1 in the thylakoid membrane, we digested thylakoid membranes with trypsin. Immunoblot analysis showed that AtBest is resistant to trypsin treatment, like the luminal protein PsbO (Figure 2E). As expected, PGRL1 was digested within 10 min, since its C- and N-termini protrude into the stroma. These results imply that the C- and N-termini, as well as the loop between TMD2 and TMD3 of the AtBest1 protein, are present in the thylakoid lumen (Figure 2F). Based on its similarity to the cBest1 and KpBest channels (Dickson et al. 2014; Yang et al. 2014), AtBest may also form a pentamer and our digestion experiment indicated that the outer entryway for ions in the AtBest channel is exposed to the chloroplast stroma, and the export aperture is located in the thylakoid lumen (Figure 2G).

Enhanced thylakoid lumen size in the *atbest* mutant

We investigated the thylakoid architecture of *atbest* using transmission electron microscopy (TEM). Although grana thylakoids had developed and were connected by the stroma lamellae in *atbest*, the grana were loosely stacked and the stroma thylakoid system was not well organized (Figure 3A). Moreover, in most of the chloroplast of *atbest*, the thylakoid lumen thickness was 20.2 ± 2.5 nm, almost twice as wide as that of the WT (10.2 ± 0.6 nm) ($P < 0.01$, Student's *t*-test, Figure 3B), indicating that AtBest is also involved in regulating thylakoid lumen size.

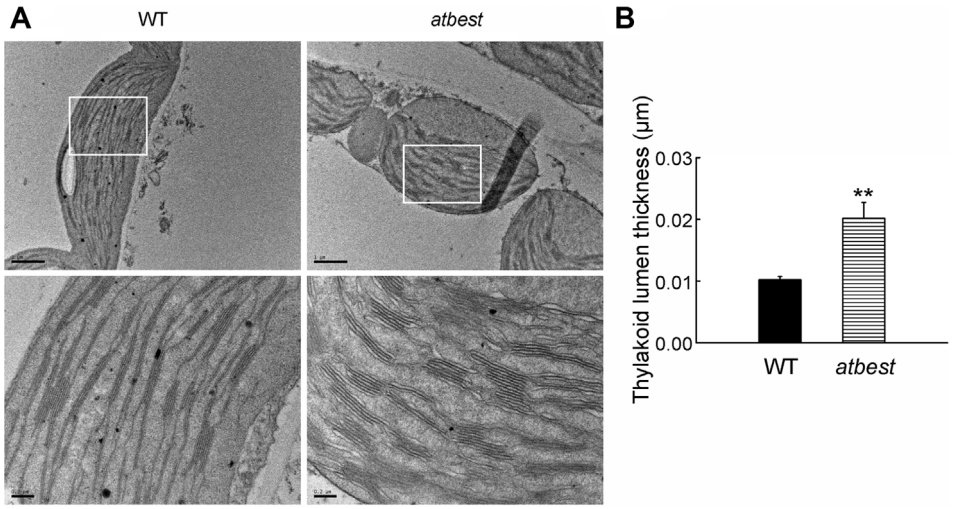

Figure 3. Electron micrographs of chloroplasts from the wild type and *atbest* mutants
(A) Chloroplasts from three-week-old wild type (WT) and *atbest* plants observed by transmission electron microscopy (bars = 1 μm). Magnified views (bars = 0.2 μm) are shown below their respective counterparts. **(B)** Thylakoid lumen thickness was calculated as described previously (Kirchhoff et al. 2011). Error bars indicate ±*SD* ($n = 15$). Asterisks indicate that thylakoid lumen thickness between WT and *atbest* differ significantly (**$P < 0.01$, Student's *t*-test).

AtBest plays an essential role in modulating pmf partitioning and NPQ induction

AtBest belongs to the bestrophin family (Figures S1, S2), which are believed to function as Cl^- channels. Furthermore, the topology of AtBest in the thylakoid indicates that AtBest may mediate Cl^- flux from chloroplast stroma into thylakoid lumen (Figure 2F, G). Due to the potential sensitivity of the pmf to changes in ion flux during photosynthesis, it is likely that the formation and/or regulation of the pmf across the thylakoid membrane would be affected by the absence of AtBest. To investigate this possibility, we performed electrochromic shift (ECS) measurements to estimate pmf and its two components, the membrane potential ($\Delta\Psi$) and H^+ gradient (ΔpH), both of which drive H^+ efflux via ATP synthase (Schreiber and Klughammer 2008). ECS is the transient red-shift of carotenoid and chlorophyll absorption bands that occurs when the thylakoid electric field forms during photosynthesis (Junge and Witt 1968; Witt 1971). Due to the quadratic and linear dependencies of ECS on the electric field, the peak of the ECS signal at approximately 515 nm (ΔA_{515}) is widely used to estimate the size of the pmf and its two components. As expected, the *atbest* mutant displayed a significant increase in total pmf and $\Delta\Psi$ compared with WT plants at low (89 μmol photons $\cdot m^{-2} \cdot s^{-1}$, $P < 0.01$, Student's *t*-test), moderate (325 μmol photons $\cdot m^{-2} \cdot s^{-1}$, $0.01 < P < 0.05$, Student's *t*-test), and high (754 μmol photons $\cdot m^{-2} \cdot s^{-1}$, $0.01 < P < 0.05$, Student's *t*-test) light intensities (Figure 4A). By contrast, a slight decrease in ΔpH was observed in the *atbest* mutant compared to WT plants at various light intensities (Figure 4A). These results imply that AtBest is essential for dissipation of $\Delta\Psi$ and modulation of pmf partitioning.

To characterize the effects of the absence of AtBest on the regulation of photosynthesis in detail, we measured NPQ induction under various light conditions. The defects in chloroplast pH homeostasis and pmf partitioning in the *atbest* mutant may result in altered NPQ induction in response to excess light. As shown in Figure 4B, induction of NPQ was less efficient in the *atbest* mutant than in WT plants within 2 min of the dark-to-light transition. However, after illumination for 2 min at low light intensity or 4 min at moderate or high light intensities, the NPQ levels in *atbest* were almost identical to those in WT plants (Figure 4B). These results imply that the NPQ capacity is not affected in the mutant, but that the induction of NPQ is kinetically less efficient. It is likely that the AtBest-mediated influx of Cl^- into the thylakoid lumen plays a critical role in rapid formation of ΔpH gradient via dissipation of $\Delta\Psi$, as observed in our ECS analysis (Figure 4A).

The rapid decay of ECS signals after illumination (g_H^+) reflects the H^+ conductivity of the thylakoid membrane through ATP synthase and can be used to evaluate ATP synthase activity (Schreiber and Klughammer 2008). Since the two components of pmf are thermodynamically equivalent driving forces of ATP synthase, we also investigated the effects of AtBest deletion on the ECS parameter g_H^+ (Figure 4C). Unexpectedly, g_H^+ was slightly reduced in the *atbest* mutant at low, moderate, and high light intensities (Figure 4C), although the total pmf was enhanced (Figure 4A). Perhaps the altered thylakoid structure in *atbest* affects the movement of H^+ in the thylakoid lumen or, more directly, affects the activity of ATP synthase. In the presence of the H^+/K^+ exchanger nigericin, which is usually used to dissipate ΔpH without affecting $\Delta\Psi$, the g_H^+ was reduced in both WT and *atbest* plants, as expected (Figure 4C). In contrast to our finding that the g_H^+ was slightly lower in *atbest* than in WT in the absence of nigericin (Figure 4C), the g_H^+ in the *atbest* mutant was slightly higher than that in WT plants in the presence of nigericin, especially under high light irradiance (Figure 4C, $P < 0.01$, Student's *t*-test). Perhaps this result is

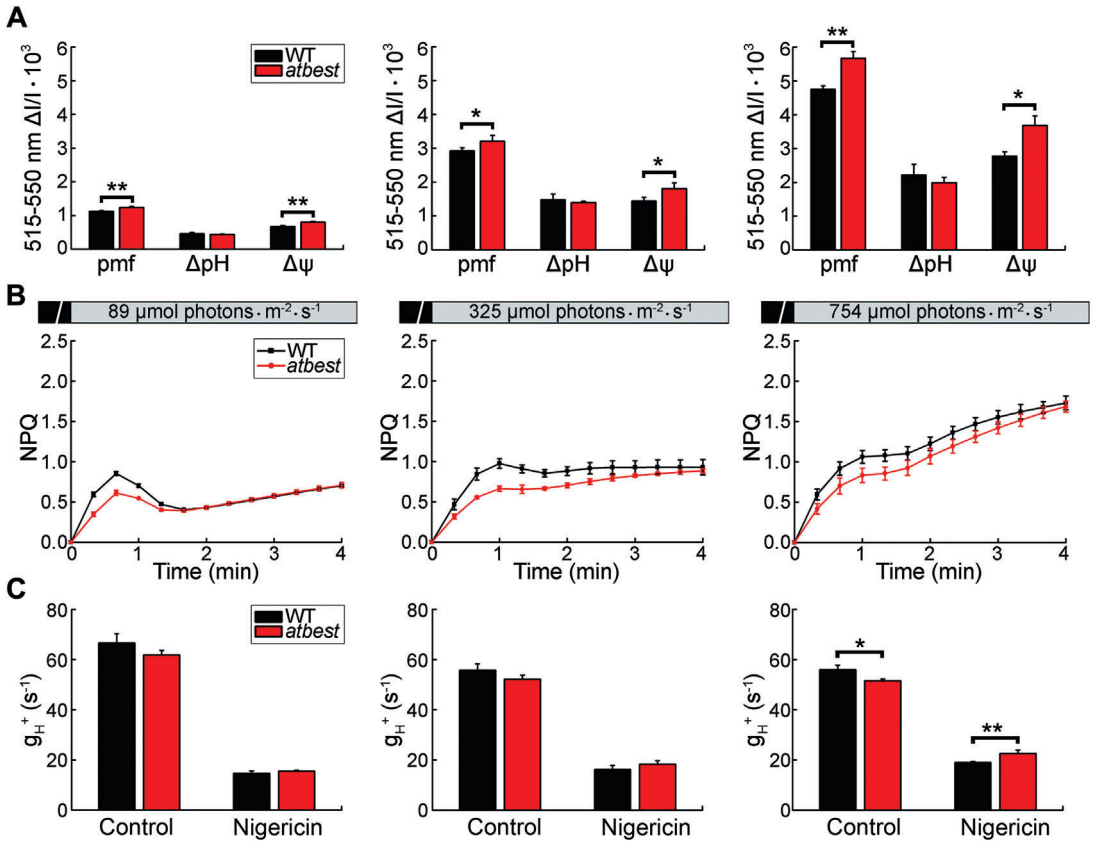

Figure 4. AtBest plays an essential role in modulating pmf partitioning and NPQ induction
(A) The proton motive force (pmf) across the thylakoid membrane. The pmf was determined based on the slow relaxation phase of the ECS signal after illumination with light intensities of 89 (left), 325 (middle), or 754 (right) μmol photons · m^{-2} · s^{-1} for 10 min. The pmf was further partitioned into the pH gradient component (ΔpH) and the electric field component (ΔΨ). Asterisks indicate where WT and *atbest* differ significantly ($^{*}0.01 < P < 0.05$, $^{**}P < 0.01$, Student's *t*-test). **(B)** NPQ induction curves of wild type (WT) and *atbest* mutant plants. NPQ was determined upon illumination with light intensities of 89, 325, or 754 μmol photons · m^{-2} · s^{-1}. NPQ was calculated as (Fm-Fm′)/Fm′. **(C)** H^+ conductivity via ATP synthase ($g_H{}^+$) in WT and *atbest* plants. $g_H{}^+$ was inferred from the fast decay kinetics of the ECS signal during a short dark interval after a 10-min illumination with 89 (left), 325 (middle), or 754 (right) μmol photons · m^{-2} · s^{-1} light intensity. Asterisks indicate where WT and *atbest* differ significantly ($^{*}0.01 < P < 0.05$, $^{**}P < 0.01$, Student's *t*-test). All of the data are presented as the means ± *SD* (n = 3).

due to the ΔΨ component of pmf being higher in the *atbest* mutant than in WT plants (Figure 4A), which results in a higher driving force for ATP synthase in *atbest* than in the WT.

AtBest is required for photoprotection under fluctuating light conditions and in the field

To investigate the physiological role of AtBest, we exposed plants to alternating cycles of 60 s of low light (50 μmol photons · m^{-2} · s^{-1}) and 120 s of high light (700 μmol photons · m^{-2} · s^{-1}) and measured NPQ induction. As shown in Figure 5A, NPQ induction was less efficient during the transition from low to high light (Figure 5A). Since NPQ is thought to play a significant role in protecting PSII from photoinhibition caused by absorbed excess light, it is likely that Atbest is required for photoprotection under fluctuating light conditions. Indeed, the ratio of variable fluorescence to maximum fluorescence (Fv/Fm), which reflects the maximum potential capacity of the photochemical reactions of PSII, was reduced in *atbest* plants grown in the field compared with WT plants (Figure 5B). On rainy days, the WT and mutant plants exhibited similar levels of photoinhibition. However, on sunny days, stronger photoinhibition was observed in *atbest* compared to WT plants. No difference in Fv/Fm was found between *atbest* and WT plants grown in the greenhouse (Figure 5B). We also investigated the light intensity dependence of NPQ to analyze subtle defects in the photosynthetic activity of the *atbest* mutant grown in the greenhouse or field (Figures S4, S5). NPQ was not affected in mutant plants grown in the greenhouse under constant low light intensity (Figure 5C, E), which is consistent with the finding that there was no difference in Fv/Fm level between WT and *atbest* plants (Figure 5B). For plants grown in the field, however, NPQ levels were significantly lower in *atbest* than in the WT at light intensities of more than 300 μmol photons · m^{-2} · s^{-1} (Figure 5D, F, $P < 0.01$, Student's *t*-test). These results, together with the reduced Fv/Fm observed in the *atbest* mutant grown in the field, highlight that AtBest is important for photoprotection of plants in the field.

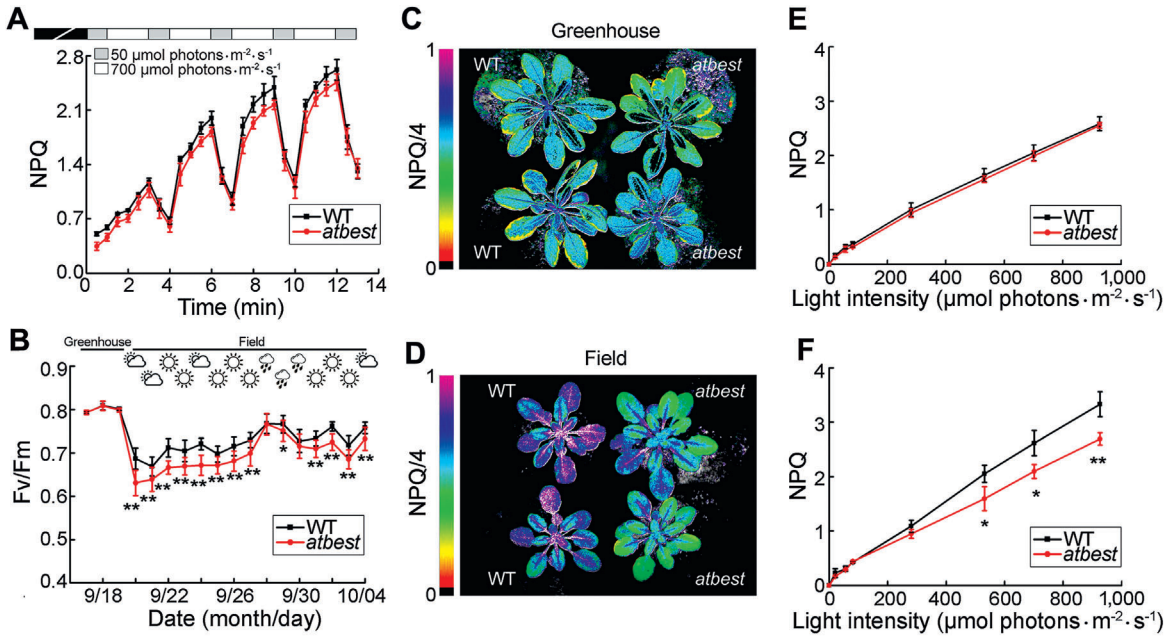

Figure 5. AtBest is required for efficient NPQ induction under fluctuating light conditions and in the field
(A) Induction of NPQ in fluctuating light. Dark-adapted plants were illuminated with fluctuating light of 50 μmol photons · m^{-2} · s^{-1} for 1 min and 700 μmol photons · m^{-2} · s^{-1} for 2 min, and NPQ was measured. Means ± *SD* (n = 3). **(B)** Photoinhibition in the field. Three-week-old wild-type (WT) and *atbest* plants grown in the greenhouse were shifted to the field (from 20 Sept to 4 Oct, 2015), and Fv/Fm was measured each day at 2:00 PM. Weather conditions for each day are indicated with symbols (sunny, cloudy, and rainy). Asterisks indicate that Fv/Fm is significantly lower in *atbest* than in the WT ($^{*}0.01 < P < 0.05$, $^{**}P < 0.01$, Student's *t*-test). **(C, D)** Images of NPQ levels at a light intensity of 701 μmol photons · m^{-2} · s^{-1} for wild-type and mutant plants grown in the greenhouse (**C**) or in the field (**D**). Light intensity dependence of NPQ was measured using an IMAGING-PAM fluorometer with a series of light intensities (21, 56, 81, 281, 531, 701, and 926 μmol photons · m^{-2} · s^{-1}). The NPQ image was captured after 2 min illumination with 701 μmol photons · m^{-2} · s^{-1} red light. Signal intensities for NPQ/4 are indicated according to the color scale from 0 to 1.0 on the left. **(E, F)** Light curves of NPQ for WT and *atbest* plants grown in the greenhouse (**E**) or in the field (**F**). The values were deduced based on images of NPQ at various light intensities (Figure S4). Asterisks indicate where WT and *atbest* differ significantly ($^{*}0.01 < P < 0.05$, $^{**}P < 0.01$, Student's *t*-test) **(F)**.

DISCUSSION

In this study, we identified and characterized a potential Cl^- channel, AtBest, in chloroplasts (Figure 1). AtBest may mediate Cl^- transport from the chloroplast stroma into the thylakoid lumen when photosynthetic electron transport is activated, which is essential for dissipation of the electric field gradient across the thylakoid (Figures 2–4). Based on our results and earlier reports (Checchetto et al. 2012; Carraretto et al. 2013; Armbruster et al. 2014; Kunz et al. 2014; Herdean et al. 2016), we propose a model for the regulation of thylakoid pmf in the chloroplast (Figure 6). Activation of photosynthetic electron transport, including linear electron transport and cyclic electron transport around PSI, results in the accumulation of H^+ in the thylakoid lumen, leading to the formation of a large $\Delta\Psi$ component. The K^+ channel AtTPK3 and Cl^- channel AtBest are activated to mediate the efflux of K^+ and influx of Cl^-, respectively. Under certain conditions, such as a shift from high light to low light or darkness, the H^+/K^+ antiporter KEA3 mediates K^+ uptake into the thylakoid lumen. The identity of the molecule responsible for Cl^- efflux is still unclear. Since the CLCe is the only CLC family member located on the thylakoid membrane, this molecule may function as an H^+/Cl^- antiporter or Cl^- channel that mediates the efflux of Cl^- from the thylakoid lumen (Marmagne et al. 2007; Lv et al. 2009; Barbier-Brygoo et al. 2011; Herdean et al. 2016). Through this type of ion counterbalancing, electroneutrality in the thylakoid lumen is maintained and partitioning of the pmf between $\Delta\Psi$ and ΔpH is precisely regulated to ensure the balance of efficient light utilization and dissipation of excess light excitation energy (Figure 6).

AtBest is located in the thylakoid membrane and is a bestrophin family protein (Figures 2, S1, S2). In addition to occurring in mammals, bestrophin proteins are ubiquitous in phototrophs, including angiosperms, bryophytes, and cyanobacteria (Figure S2). Like mammalian bestrophin proteins, bestrophin proteins from phototrophs also contain four transmembrane domains, suggesting that these homologs share a similar structure (Figures 2F, G, S2). In 1988, Schönknecht and coworkers recorded a voltage-dependent Cl^- channel with a high unitary conductance (~65 pS, at 30 mM Cl^-) in the thylakoid membranes by patch-clamp technology (Schönknecht et al. 1988). The question now arises whether AtBest is responsible for the Cl^- channel activity detected by Schönknecht and coworkers in 1988. Mammalian bestrophin proteins usually have a very low

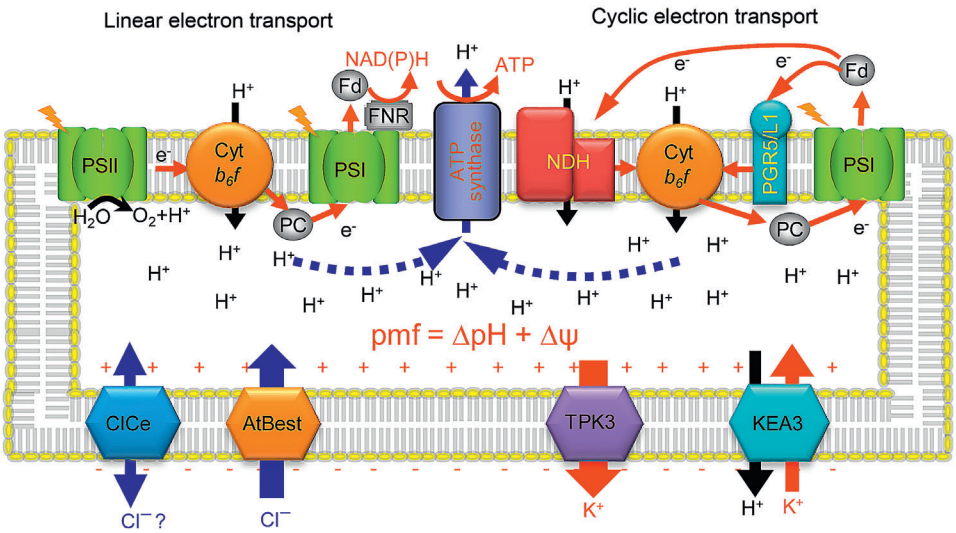

Figure 6. Possible model for Cl^- and K^+ flux across the thylakoid membrane during photosynthesis
Activation of linear and cyclic electron transport leads to the formation of a proton motive force across the thylakoid membrane, which is composed of two components, $\Delta\Psi$ and ΔpH. To dissipate $\Delta\Psi$ rapidly, the K^+ channel AtTPK3 and Cl^- channel AtBest are activated to mediate K^+ efflux and Cl^- influx, respectively. Under certain conditions (such as a shift from high light to low light or darkness), the H^+/K^+ antiporter KEA3 mediates K^+ uptake into the thylakoid lumen. The molecule responsible for Cl^- efflux is still unclear; ClCe protein may be involved in this process.

conductance (0.2–2 pS) and belong to the Ca^{2+}-activated anion channel family (Sun et al. 2002; Fischmeister and Hartzell 2005; Chien et al. 2006; Pifferi et al. 2006). Thus, AtBest is unlikely to be responsible for the Cl^- channel activity detected in thylakoid membranes by Schönknecht and coworkers. However, protein alignment and phylogenetic tree analyses showed that amino acids in phototrophic bestrophin proteins show high diversity compared with their counterparts in mammals (Figures 2A, S1, S2). For example, the residues forming the Ca^{2+} sensing apparatus in animal bestrophin are not conserved in AtBest (Dickson et al. 2014; Figure S1), suggesting that Ca^{2+} is not required for AtBest channel activation in chloroplasts. These facts suggest that, during evolution, bestrophin proteins in phototrophs may have acquired different electrophysiological properties from those in mammals. The mechanism of activation and regulation of AtBest should be investigated in future studies.

Although the *atbest* mutant showed no visible phenotype under greenhouse conditions, a stronger photoinhibition phenomenon was observed in *atbest* mutant plants grown in the field (Figure 5). How does AtBest protect higher plants from photoinhibition in the field? A significant increase in $\Delta\Psi$ and a slight decrease in ΔpH were observed in the absence of AtBest, resulting in an increase in total pmf (Figure 4). High $\Delta\Psi$ is thought to promote the recombination of $P680^+$ with Phe^- or Q_A^- in PSII, thereby enhancing the formation of $^1O_2$, which is highly active and toxic to the PSII complex (Bennoun 1994). Furthermore, activation of NPQ was less efficient in *atbest* when the plants were transiently shifted from low light to high light intensities and in the field (Figure 5). Energy-dependent non-photochemical quenching (qE, the main component of NPQ) is also critical for resistance against photoinhibition by reducing the formation of $^1O_2$ in PSII (Li et al. 2000; Müller et al. 2001). Thus, enhanced formation of $^1O_2$ in PSII may be one reason for the stronger photoinhibition detected in *atbest* plants.

The thylakoid luminal compartment was significantly larger in *atbest* than in WT plants (Figure 3), which may also lead to the stronger photoinhibition observed in the *atbest* mutant. A similar phenotype was observed in sunlight-grown *Monstera* plants (Demmig-Adams et al. 2015) and in *Arabidopsis* plants treated with moderate light (Kirchhoff et al. 2011; Tsabari et al. 2015). Altered luminal volume is believed to play critical roles in modulating photosynthetic electron transfer, photoprotection, and efficient repair of damaged photosystem II. Ion flux through the thylakoid membrane during photosynthesis may modify the size of the thylakoid lumen, and net influx of Cl^- into the lumen may lead to its swelling (Tsabari et al. 2015). However, our results show that the thylakoid lumen was also swollen in *atbest* (Figure 3). This finding suggests that other ions or chemical compounds enter the thylakoid lumen instead of Cl^-. Furthermore, several aquaporins were postulated to be present in the thylakoid membrane, which may be required for rapid regulation of lumen volume following ion flux activity during photosynthesis (Beebo et al. 2013). The finding that the lumen was enlarged in the *atbest* mutant suggests that, in coordination with other channels and transporters, AtBest is critical for the regulation of lumen volume.

In summary, we discovered a novel protein, AtBest, in the thylakoid using forward genetics and unraveled its physiological function in fine-tuning of photosynthesis of higher plants. Probably by mediating the influx of Cl^- into the thylakoid lumen during photosynthesis, AtBest directly reduces the $\Delta\Psi$ component of pmf and indirectly influences the activation of nonphotochemical dissipation of excess absorbed light, as well as thylakoid structure and, ultimately, plant fitness.

MATERIALS AND METHODS

Plant materials and growth conditions

The homozygous *atbest1-2* (GK-796C09) and *atbest2-1* (SALK_114715C) mutants of *Arabidopsis thaliana* (Columbia, Col-0) obtained from the ABRC (http://abrc.osu.edu) and were verified by PCR. Plants were grown in soil under a 12-h-light/12-h-dark cycle at a light intensity of 80 μmol photons $\cdot m^{-2} \cdot s^{-1}$ in a growth chamber at 23 °C. To investigate the fitness of the mutant in the field, 3-week-old *atbest* and WT plants grown in the growth chamber were transferred to the field and grown for 2 weeks. The light intensities and temperature were recorded (Figure S5) and the Fv/Fm values of the plants were measured at 2:00 PM each day. For complementation analysis, cDNA coding regions of *AtBest1* (*At3g61320*) or *AtBest2* (*At2g45870*) were cloned into the plant expression vector pBI121. The resulting vectors were introduced into the *atbest1-1 atbest2-1* double mutant (also referred to as the *atbest* mutant), respectively, by the floral-dip method (Clough and Bent 1998). Transgenic seeds were selected on Murashige and Skoog medium with 50 μg/mL kanamycin, and the transformed seedlings were further confirmed by chlorophyll fluorescence analysis.

Nucleic acid analysis

The *atbest1-1* mutant gene was mapped according to the previously described method (Lukowitz et al. 2000). Candidate genes in the mapped region were analyzed through high-throughput sequencing. Total RNA was isolated from leaves using Trizol reagent (Invitrogen, http://www.thermofisher.com). Reverse-transcription PCR (RT-PCR) was carried out using gene-specific primers, and the *ACT7* gene (*AT5G09810*) was used as an internal control. Quantitative real-time RT-PCR was performed using UltraSYBR Mixture.

Chlorophyll fluorescence measurements

Chlorophyll Fluorescence measurements were performed using an IMAGING-PAM fluorometer or a MINI-PAM portable chlorophyll fluorometer (Walz, Effeltrich, Germany). Fv/Fm and NPQ were calculated as previously described (Munekage et al. 2002). Light intensity dependence of NPQ was measured using an IMAGING-PAM fluorometer with a series of light intensities (21, 56, 81, 281, 531, 700, and 926 μmol photons $\cdot m^{-2} \cdot s^{-1}$). The NPQ image was captured after 2 min illumination with various intensities of red light (Figure S4).

Chloroplast fractionation and immunoblotting

Intact chloroplasts, thylakoid membranes, and stromal proteins were isolated as previously described (Peng et al. 2010). To prepare chloroplast envelope membrane, intact chloroplasts were ruptured via a freeze–thaw cycle and pure envelope membranes were isolated by sucrose gradient centrifugation (Keegstra and Yousif 1988; Froehlich et al. 2003). For immunoblotting, the proteins were separated by Laemmli-SDS-PAGE or SDS-urea-PAGE and transferred to nitrocellulose membranes. Proteins were detected with specific antibodies in TTBS buffer with 1% skimmed milk and visualized by the chemiluminescence method using LuminoGraph WSE-6100 (ATTO Corporation, http://www.atto.co.jp/).

ECS measurements

Electrochromic shift measurements were performed using the Dual-PAM-100 (Walz, Effeltrich, Germany) with the P515/535 module (Schreiber and Klughammer 2008). Plants were dark adapted overnight and illuminated for 10 min at light intensities of 89, 325, and 754 μmol photons $\cdot m^{-2} \cdot s^{-1}$. After illumination, inverse electrochromic band-shift kinetics was recorded for 1 min. Values for pmf, $\Delta\Psi$, and ΔpH were calculated as previously described (Schreiber and Klughammer 2008). The H^+ conductivity through ATP synthase ($g_H{}^+$) was measured as previously described (Kanazawa and Kramer 2002).

Other methods

Subcellular localization of AtBest was analyzed as described by Zhong et al. (2013). Polyclonal antibodies were raised in rabbit with purified recombinant AtBest1 (amino acids 180 to 410 of mature AtBest1). Plastid-targeting signal (cTP) and transmembrane domains of AtBest were predicted by ChloroP analysis (http://www.cbs.dtu.dk/services/ChloroP) and TMHMM software (http://www.cbs.dtu.dk/services/TMHMM-2.0), respectively. The overall structure of AtBest1 was predicted by SwissModel (http://swissmodel.expasy.org) using KpBest as a template. Sequence alignment of AtBest was performed with ClustalW2. The phylogenetic tree of bestrophin superfamily proteins was constructed using the neighbor-joining method in the MEGA5 software suite (Tamura et al. 2011).

ACKNOWLEDGEMENTS

We are grateful to Dr. Chunyan Zhang, and Fengqin Dong for their technical assistance. This work was supported by the National Natural Science Foundation of China (31322007 and 31570239) and the Hundred Talents Program of the Chinese Academy of Sciences.

AUTHOR CONTRIBUTIONS

Z.D., F.K. and L.Z. performed most of the experiments. W.L. isolated the *atbest1-1* mutant. J.Z. carried out the GFP experiments. Z.D. and L.Z. drafted the manuscript. L.P. designed the experiment, supervised the study, and revised the manuscript.

REFERENCES

Armbruster U, Carrillo LR, Venema K, Pavlovic L, Schmidtmann E, Kornfeld A, Jahns P, Berry JA, Kramer DM, Jonikas MC (2014) Ion antiport accelerates photosynthetic acclimation in fluctuating light environments. **Nat Commun** 5: 5439

Barbier-Brygoo H, De Angeli A, Filleur S, Frachisse JM, Gambale F, Thomine S, Wege S (2011) Anion channels/transporters in plants: From molecular bases to regulatory networks. **Annu Rev Plant Biol** 62: 25–51

Beebo A, Mathai JC, Schoefs B, Spetea C (2013) Assessment of the requirement for aquaporins in the thylakoid membrane of plant chloroplasts to sustain photosynthetic water oxidation. **FEBS Lett** 587: 2083–2089

Bennoun P (1994) Chlororespiration revisited: Mitochondrial-plastid interactions in *Chlamydomonas*. **Biochim Biophys Acta** 1186: 59–66

Carraretto L, Formentin E, Teardo E, Checchetto V, Tomizioli M, Morosinotto T, Giacometti GM, Finazzi G, Szabò I (2013) A thylakoid-located two-pore K^+ channel controls photosynthetic light utilization in plants. **Science** 342: 114–118

Checchetto V, Segalla A, Allorent G, La Rocca N, Leanza L, Giacometti GM, Uozumi N, Finazzi G, Bergantino E, Szabò I (2012) Thylakoid potassium channel is required for efficient photosynthesis in cyanobacteria. **Proc Natl Acad Sci USA** 109: 11043–11048

Chien LT, Zhang ZR, Hartzell HC (2006) Single Cl^- channels activated by Ca^{2+} in *Drosophila* S2 cells are mediated by bestrophins. **J Gen Physiol** 128: 247–259

Clough SJ, Bent AF (1998) Floral dip: A simplified method for *Agrobacterium*-mediated transformation of *Arabidopsis thaliana*. **Plant J** 16: 735–743

Cruz JA, Sacksteder CA, Kanazawa A, Kramer DM (2001) Contribution of electric field ($\Delta\Psi$) to steady-state transthylakoid proton motive force (pmf) in vitro and in vivo. Control of pmf parsing into $\Delta\Psi$ and ΔpH by ionic strength. **Biochemistry** 40: 1226–1237

Demmig-Adams B, Muller O, Stewart JJ, Cohu CM, Adams WW (2015) Chloroplast thylakoid structure in evergreen leaves employing strong thermal energy dissipation. **J Photoch Photobio B** 152: 357–366

Dickson VK, Pedi L, Long SB (2014) Structure and insights into the function of a Ca^{2+}-activated Cl^- channel. **Nature** 516: 213–218

Fischmeister R, Hartzell HC (2005) Volume-sensitivity of the bestrophin family of chloride channels. **J Physiol** 562: 477–491

Froehlich JE, Wilkerson CG, Ray WK, McAndrew RS, Osteryoung KW, Gage DA, Phinney BS (2003) Proteomic study of the *Arabidopsis thaliana* chloroplastic envelope membrane utilizing alternatives to traditional two-dimensional electrophoresis. **J Proteome Res** 2: 413–425

Herdean A, Nziengui H, Zsiros O, Solymosi K, Garab G, Lundin B, Spetea C (2016) The *Arabidopsis* thylakoid chloride channel AtCLCe functions in chloride homeostasis and regulation of photosynthetic electron transport. **Front Plant Sci** 7: 115

Hind G, Nakatani HY, Izawa S (1974) Light-dependent redistribution of ions in suspensions of chloroplast thylakoid membranes. **Proc Natl Acad Sci USA** 71: 1484–1488

Hope AB, Valente P, Matthews DB (1994) Effects of pH on the kinetics of redox reactions in and around the cytochrome *bf* complex in an isolated system. **Photosynth Res** 42: 111–120

Johnson MP, Ruban AV (2014) Rethinking the existence of a steady-state $\Delta\Psi$ component of the proton motive force across plant thylakoid membranes. **Photosynth Res** 119: 233–242

Junge W, Witt HT (1968) On the ion transport system in photosynthesis: Investigations on a molecular level. **Z Naturforsch B** 23: 244–254

Kanazawa A, Kramer DM (2002) In vivo modulation of nonphotochemical exciton quenching (NPQ) by regulation of the chloroplast ATP synthase. **Proc Natl Acad Sci USA** 99: 12789–12794

Keegstra K, Yousif AE (1988) Isolation and characterization of chloroplast envelope membranes. **Method Enzymol** 118: 316–325

Kirchhoff H, Hall C, Wood M, Herbstová M, Tsabari O, Nevo R, Charuvib D, Shimonic E, Reich Z (2011) Dynamic control of protein diffusion within the granal thylakoid lumen. **Proc Natl Acad Sci USA** 108: 20248–20253

Kramer DM, Cruz JA, Kanazawa A (2003) Balancing the central roles of the thylakoid proton gradient. **Trends Plant Sci** 8: 27–32

Kunz HH, Gierth M, Herdean A, Satoh-Cruz M, Kramer DM, Spetea C, Schroeder JI (2014) Plastidial transporters KEA1, −2, and −3 are essential for chloroplast osmoregulation, integrity, and pH regulation in *Arabidopsis*. **Proc Natl Acad Sci USA** 111: 7480–7485

Li XP, BjoÈrkman O, Shih C, Grossman AR, Rosenquist M, Jansson S, Niyogi KK (2000) A pigment-binding protein essential for regulation of photosynthetic light harvesting. **Nature** 403: 391–395

Lukowitz W, Gillmor CS, Scheible WR (2000) Positional cloning in *Arabidopsis*. Why it feels good to have a genome initiative working for you. **Plant Physiol** 123: 795–806

Lv Q, Tang R, Liu H, Gao X, Li Y, Zheng H, Zhang H (2009) Cloning and molecular analyses of the *Arabidopsis thaliana* chloride channel gene family. **Plant Sci** 176: 650–661

Marmagne A, Vinauger-Douard M, Monachello D, de Longevialle AF, Charon C, Allot M, Rappaport F, Wollman FA, Barbier-Brygoo H, Ephritikhine G (2007) Two members of the *Arabidopsis* CLC (chloride channel) family, AtCLCe and AtCLCf, are associated with thylakoid and Golgi membranes, respectively. **J Exp Bot** 58: 3385–3393

Milenkovic VM, Langmann T, Schreiber R, Kunzelmann K, Weber BH (2008) Molecular evolution and functional divergence of the bestrophin protein family. **BMC Evol Biol** 8: 72

Mitchell P (1961) Coupling of phosphorylation to electron and hydrogen transfer by a chemi-osmotic type of mechanism. **Nature** 191: 144–148

Mitchell P (1966) Chemiosmotic coupling in oxidative and photosynthetic phosphorylation. **Biol Rev** 41: 445–502

Monachello D, Allot M, Oliva S, Krapp A, Daniel-Vedele F, Barbier-Brygoo H, Ephritikhine G (2009) Two anion transporters AtClCa and AtClCe fulfill interconnecting but not redundant roles in nitrate assimilation pathways. **New Phytol** 183: 88–94

Müller P, Li XP, Niyogi KK (2001) Non-photochemical quenching. A response to excess light energy. **Plant Physiol** 125: 1558–1566

Munekage Y, Hojo M, Meurer J, Endo T, Tasaka M, Shikanai T (2002) PGR5 is involved in cyclic electron flow around photosystem I and is essential for photoprotection in *Arabidopsis*. **Cell** 110: 361–371

Niyogi KK (1999) Photoprotection revisited: Genetic and molecular approaches. **Annu Rev Plant Biol** 50: 333–359

Peng L, Cai W, Shikanai T (2010) Chloroplast stromal proteins, CRR6 and CRR7, are required for assembly of the NAD(P)H dehydrogenase subcomplex A in *Arabidopsis*. **Plant J** 63: 203–211

Petrukhin K, Koisti MJ, Bakall B, Li W, Xie G, Marknell T, Sandgren O, Forsman K, Holmgren G, Andreasson S, Vujic M, Bergen A, McGarty-Dugan V, Figueroa D, Austin CP, Metzker ML, Caskey CT, Wadelius C (1998) Identification of the gene responsible for best macular dystrophy. **Nat Genet** 19: 241–247

Pifferi S, Pascarella G, Boccaccio A, Mazzatenta A, Gustincich S, Menini A, Zucchelli S (2006) Bestrophin-2 is a candidate calcium-activated chloride channel involved in olfactory transduction. **Proc Natl Acad Sci USA** 103: 12929–12934

Pottosin II, Schönknecht G (1995) Patch clamp study of the voltage-dependent anion channel in the thylakoid membrane. **J Membrane Biol** 148: 143–156

Pottosin II, Schönknecht G (1996) Ion channel permeable for divalent and monovalent cations in native spinach thylakoid membranes. **J Membrane Biol** 152: 223–233

Schönknecht G, Hedrich R, Junge W, Raschke K (1988) A voltage-dependent chloride channel in the photosynthetic membrane of a higher plant. **Nature** 336: 589–592

Schreiber U, Klughammer C (2008) New accessory for the Dual-PAM-100: The P515/535 module and examples of its application. **PAN** 1: 1–10

Sun H, Tsunenari T, Yau KW, Nathans J (2002) The vitelliform macular dystrophy protein defines a new family of chloride channels. **Proc Natl Acad Sci USA** 99: 4008–4013

Tamura K, Peterson D, Peterson N, Stecher G, Nei M, Kumar S (2011) MEGA5: Molecular evolutionary genetics analysis using maximum likelihood, evolutionary distance, and maximum parsimony methods. **Mol Biol Evol** 28: 2731–2739

Tsabari O, Nevo R, Meir S, Carrillo LR, Kramer DM, Reich Z (2015) Differential effects of ambient or diminished CO_2 and O_2 levels on thylakoid membrane structure in light-stressed plants. **Plant J** 81: 884–894

Witt HT (1971) Coupling of quanta, electrons, fields, ions and phosphorylation in the functional membrane of photosynthesis. Results by pulse spectroscopic methods. **Q Rev Biophys** 4: 365–477

Yang T, Liu Q, Kloss B, Bruni R, Kalathur RC, Guo Y, Kloppmann E, Rost B, Colecraft HM, Hendrickson WA (2014) Structure and selectivity in bestrophin ion channels. **Science** 346: 355–359

Zhong L, Zhou W, Wang H, Ding S, Lu Q, Wen X, Peng L, Zhang L, Lu C (2013) Chloroplast small heat shock protein HSP21 interacts with plastid nucleoid protein pTAC5 and is essential for chloroplast development in *Arabidopsis* under heat stress. **Plant Cell** 25: 2925–2943

SUPPORTING INFORMATION

Additional supporting information may be found in the online version of this article at the publisher's web-site.

Figure S1. Sequence alignment of bestrophin-like proteins from phototrophic organisms

Sequences were obtained from GenBank (http://www.ncbi.nlm.nih.gov/) or Phytozome (http://www.phytozome.net/) (AtBest1, *Arabidopsis thaliana*, AT3G61320; AtBest2, AT2G45870; GmaBest1, *Glycine max*, Glyma03g01281; GmaBest2, *Glycine max*, Glyma07g07830; OsaBest1, *Oryza sativa*, Os03g01570; ZmaBest1, *Zea mays*, GRMZM2G114469; SmoBest1, *Selaginella moellendorffii*, XP_002962243; PptBest1, *Physcomitrella patens*, Pp1s13_344V6; CreBest1, *Chlamydomonas reinhardtii*, Cre16.g663400; SynBest1, *Synechocystis* sp. PCC 6803, sll1024) and aligned with ClustalW2. The predicted cleavage site of AtBest1 is indicated by an arrowhead above the sequence. Four transmembrane domains (TMD1-4) are shown in boxes. Identical amino acids are shown with white letters on a black background, and similar amino acids are indicated with black letters on a gray background.

Figure S2. Phylogenetic tree of bestrophin superfamily proteins

Sequences of bestrophin superfamily proteins were obtained from GenBank (http://www.ncbi.nlm.nih.gov/) or Phytozome (http://www. phytozome.net/). Angiosperms, bryophytes, chlorophyta, and chordata are highlighted in green, blue, purple, and orange, respectively. Evolutionary analyses were conducted in MEGA5 using the neighbor-joining method. Bootstrap values (1000 replicates) $\geq$70% are indicated beside each branch.

Figure S3. Levels of thylakoid proteins are unaffected in *atbest*

(A) Immunodetection of thylakoid proteins from wild type (WT) and *atbest* mutants. Thylakoid membrane proteins were fractionated by 15% SDS-urea-PAGE and immunodetected using specific antibodies. Thylakoid proteins were loaded on an equal chlorophyll basis. **(B)** Blue native polyacrylamide gel electrophoresis (BN-PAGE) of thylakoid membrane protein complexes. Freshly isolated thylakoid membrane from WT and *atbest* mutants was solubilized with 1% dodecyl-β-D-maltoside (DM) and protein complexes (10 μg chlorophyll) were separated by 5–12% BN-PAGE. NDH-PSI, NDH-PSI supercomplex. **(C)** Two-dimensional (2D) BN/SDS-PAGE separation of thylakoid protein complexes. Complexes separated by BN-PAGE in the first dimension **(B)** were subjected to denaturing 2D/SDS-urea-PAGE. Proteins were stained with CBB; the identities of relevant proteins are indicated.

Figure S4. Growth phenotypes and images of light intensity dependence of NPQ

Wild-type and mutant plants were grown in the greenhouse for 5 weeks (upper) or in the greenhouse for 3 weeks and in the field for an additional 2 weeks (below). Light intensity dependence of NPQ was measured using an IMAGING-PAM fluorometer with a series of light intensities (21, 56, 81, 281, 531, 701, and 926 μmol photons $\cdot m^{-2} \cdot s^{-1}$). The NPQ image was captured after 2 min illumination with each light intensity. Signal intensities for NPQ/4 are indicated according to the color scale (0 to 1.0) on the right.

Figure S5. Light intensities and temperature in the field

Light intensity and temperature near IBCAS are recorded at 2:00 PM (from 20 Sept. to 4 Oct., 2015). Weather conditions for corresponding day are indicated with symbols (sunny, cloudy, and rainy).

Table S1. Primers used in this work